PROCEEDINGS OF SCIENCE

Development of a new compact and 2D-multiplexed Time Projection Chamber for muon tomography

M. Lehuraux,[a,*] **D. Attié,**[a] **H. Gómez,**[a] **I. Mandjavidze,**[a] **P. Mas,**[a] **S. Procureur**[a] **and M. Vandenbroucke**[a]

[a] *CEA/DRF/Irfu,*
91191 Gif-sur-Yvette, France

E-mail: marion.lehuraux@cea.fr

Muon tomography consists in using cosmic muons to probe structures in a neither invasive nor destructive way. Following the first muography of a water tower using a muon telescope based on Micro-Pattern Gaseous Detectors and developed at Commissariat à l'énergie atomique et aux énergies alternatives (CEA) Saclay in 2015, the gaseous detectors and electronics have been developed to be more robust to high variations of temperature, allowing to operate for example in Egypt for the ScanPyramids mission since 2016. More recently, simulations showed that muon telescopes based on multiplexed Micromegas detectors could also be used to detect cavities for geology studies or dismantling of nuclear facility leading to several partnerships with industrials. However, most of the muon telescopes used nowadays are based on the hodoscope approach, requiring several detectors to operate and reconstruct muon tracks with a limited angular acceptance and compacity. To expand the spectrum of applications, CEA is developing a highly pixelated and 2D-multiplexed compact Time Projection Chamber (TPC) that would allow a full track reconstruction with a quasi-isotropical angular acceptance. In addition, this detector is meant to be as compact as possible and has been designed to fit into existing boreholes. Such detectors could be installed in a network to both detect and localise structures in the underground [1].

In this work we present the design of this new detector as well as the first prototypes developments and reconstruction algorithm.

41st International Conference on High Energy physics - ICHEP2022
6-13 July, 2022
Bologna, Italy

*Speaker

PoS(ICHEP2022)853

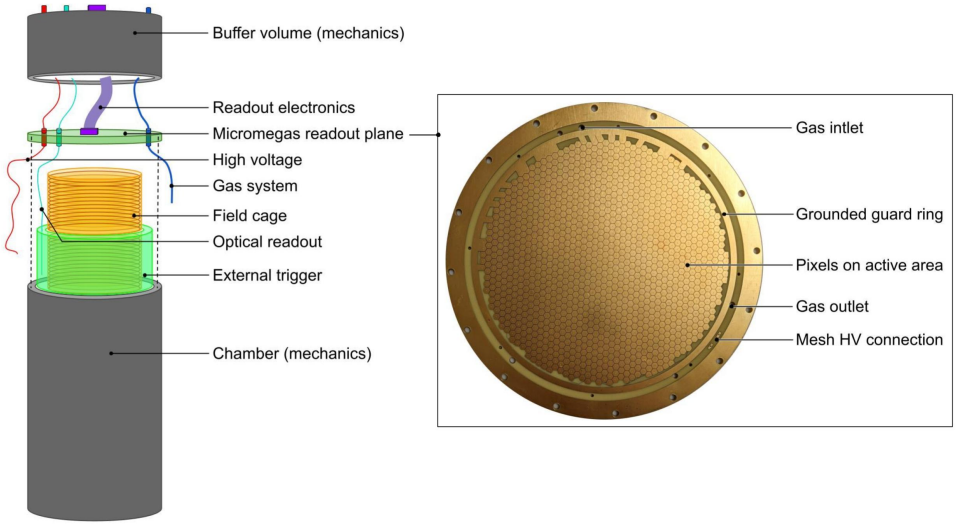

Figure 1: Schematic exploded view of D3DT detector design. A photograph of the readout plane is also annoted.

1. Detector design

The design of D3DT (Detector 3D for muon Tomography) is presented on Fig 1 and consists in a 40 cm drift cylindrical TPC read by a bulk Micromegas detector [3]. A plastic scintillator cylinder is inserted between the stainless steel chamber and field cage to serve as external trigger. The bulk Micromegas readout plane is paved by 1344 hexagonal pixels divided onto three identically mapped sectors, each one read by a DREAM [4] Application Specific Integrated Circuit (ASIC). The readout plane is 2D-multiplexed: each electronic channel is connected to between 6 and 9 pixels. The mapping is made so that 2 electronic channels are neighbours only once on each sector, theoretically ensuring the possibility to unambiguously reconstruct the tracks. A Front End Unit (FEU) card reads the three ASICs and is connected to a Intel NUC mini-PC for data acquisition. At the moment, high voltage is provided by an external Iseg SHR high voltage power supply but at term, a miniaturized version of the readout electronic and power supply should be placed in the buffer volume. The Ar-iC_4H_{10}-CF_4 (95:2:3) gas mixture is currently circulated through the detector but to facilitate underground operation, the objective would be at term to have a sealed detector. There could be a gas filtration and re-circulation unit inside a larger buffer volume as well.

2. First prototypes

Several prototypes were developed for multiple purposes, the main ones being a 5 mm drift designed to precisely characterize the Micromegas readout plane and a full size prototype to face and overcome eventual issues with the assembly, high voltage power supply or field cage.

2.1 Readout plane characterization prototypes

As further developed in the next Section, Micromegas readout plane were precisely characterized using a ^{55}Fe radioactive source. As a result, the cathode was first made out of a 20 µm

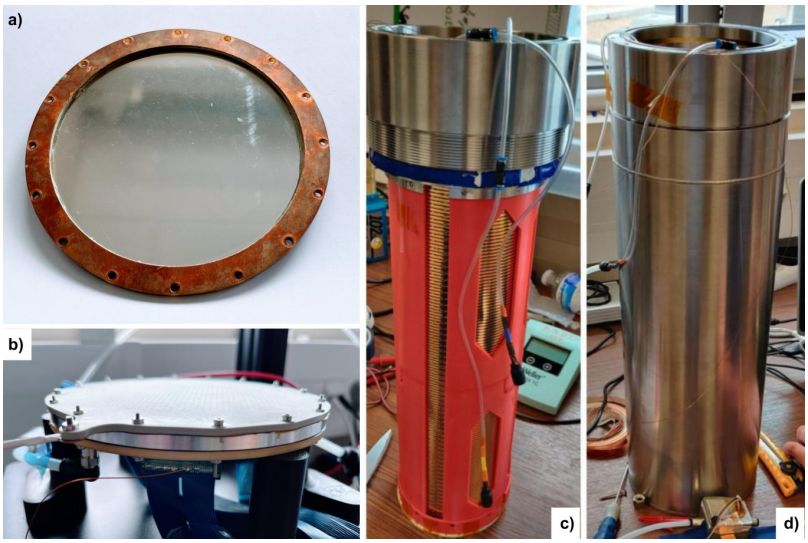

Figure 2: a) Photograph of the 20 µm thick Mylar window cathode; **b)** Thin prototype for readout plane characterization with stronger cathode design; **c)** Inner part of the full size prototype; **d)** Assembled full size prototype.

thick Mylar window illustrated in Fig 2a) allowing both the ionization of the gas in the chamber by the 5.9 keV photons and the drift field production. Later on, a stronger design of the cathode was proposed to support the Mylar foil as well as collimate the ^{55}Fe source, consisting of a plastic disk with an array of 0.75 mm diameter collimating holes with the Mylar foil glued on the internal face.

2.2 Full size prototypes

Two full-size prototypes have been built so far with different length of buffer volume. Photographs of the field cage and assembled prototype are shown on Fig 2c) and Fig 2d) respectively. First tracks were successfully observed at a preliminary stage (scintillator trigger not instrumented and cathode high voltage limited to 6 kV) and further developments are ongoing: the first full-size prototype with external trigger is expected within the next few months.

3. Readout plane characterization

An automatized test bench has been developed to precisely characterize the readout plane [2]: each intersection of 3 pixels is scanned by a ^{55}Fe source and the relative gain and energy resolution are estimated using a Gaussian fit to the 5.9 keV peak of the reconstructed spectrum. The obtained results are shown in Fig 3: one of the three sectors (top left) is particularly noisy due to a PCB manufacturing error which explains the performances degradation. A descending diagonal line can be seen on both the relative gain and energy resolution and was later attributed to a wrinkle on the Mylar foil. The rest of the readout plane presents a good uniformity of the performances with a dispersion[1] estimated below 10% for both the relative gain and energy resolution.

[1]defined as the Full Width Half Maximum (FWHM) of the Gaussian fitted distribution divided by its mean.

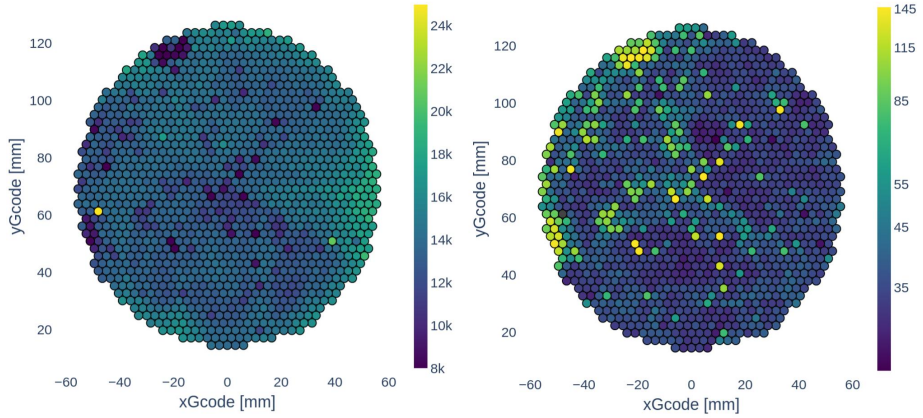

Figure 3: Left: 2D map of the relative gain in ADC; **Right:** 2D map of the energy resolution [%].

4. Track reconstruction

A specific track reconstruction algorithm is developed to accommodate for the large hit multiplicity per event and the low signal over background ratio induced by the multiplexing artefacts. Because of the limited amount and quality of the recorded data, the reconstruction algorithm is built and tested on simulated data.

4.1 Simulations

Muons are sampled following the Guan parametrization [6] and propagated through the active volume using simulations based on GEANT4 [5]. Their direction is defined by the zenithal angle θ and azimuthal angle ϕ. The active volume is defined as a cylinder of Ar-iC_4H_{10}-CF_4 (95:2:3) gas mixture and of 40 cm height and 6 cm radius to match D3DT dimensions. The hits obtained from these simulations are then projected onto D3DT readout plane: each hit represented by its coordinates $(x_{\text{hit}}, y_{\text{hit}}, z_{\text{hit}})$ contributes to the signal of the pad i centered on (x_i, y_i) defined by:

$$d_{\text{hit}\to\text{pix}} = \sqrt{(x_{\text{hit}} - x_i)^2 + (y_{\text{hit}} - y_i)} < h$$

where h is the radius of the circle inscribed in the hexagonal pixel. The energies deposited by each hit contributing to the signal collected on pixel i are summed up while the z_{hit} are averaged. Finally, in order to simulate the time digitization introduced by the readout electronics, a Gaussian smearing is applied to $z_i = \langle z_{\text{hit}} \rangle$ that is then binned. The signal of pixel i is duplicated to each pixel read by the same electronic channel.

4.2 Reconstruction algorithm

The track reconstruction algorithm developed here heavily relies on the RANSAC algorithm [7] with additionnal steps to improve the signal over background ratio beforehand thus improving the performances. To achieve this, several steps are followed:

1. **Selection of a point of reference:** this point should be part of the physical track and will be a point of reference for the next step.

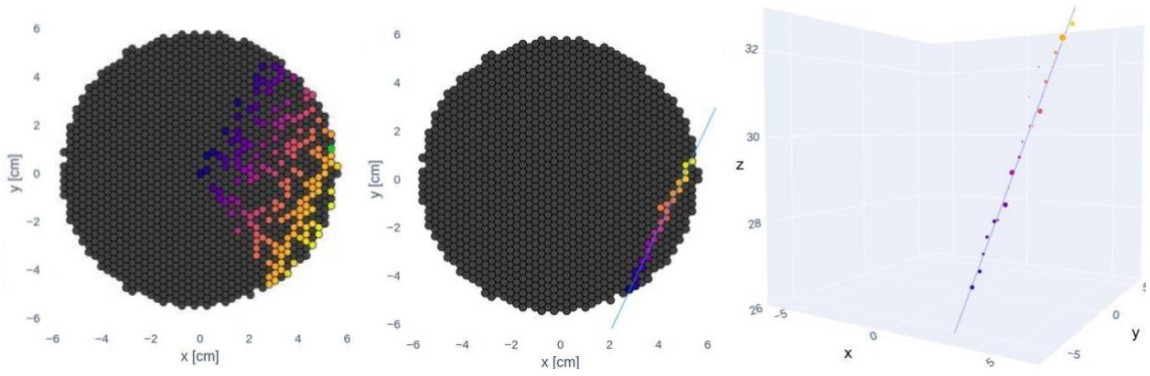

Figure 4: Left: Raw event display. The point of reference is highlighted in green and the color indicates the value of the angular selection variable introduced in Step 2; **Middle:** 2D projection of the final 3D reconstruction. Color indicates the value of the z coordinate; **Right:** Final 3D reconstruction. Maker size is proportional to the deposited energy.

2. **2D selection of a favored direction:** assuming that the point of reference is a physical hit, a gross selection is applied on the 2D data set selecting the direction containing the more hits. An angular selection variable is computed as the distance to this favored direction.
3. **First 3D-RANSAC fit to pre-selected data:** the pre-selected data set is fitted using a 3D-RANSAC algorithm.
4. **3D selection based on first RANSAC residuals:** the distance of each point to the model extracted from the first RANSAC fit is used as new selection variable which, this time, takes into account the three dimensions.
5. **Second 3D-RANSAC to reconstruct the track:** the final data set is fitted by a 3D-RANSAC algorithm to finally reconstruct the track direction.

An example of reconstructed track is shown in Fig 4 at different stages of the process.

4.3 Performances

The total reconstruction efficiency $\varepsilon_{\text{reco}}$, defined as the ratio between the number of tracks reconstructed and simulated, is estimated as the product of the efficiencies of each individual step and yields $\varepsilon_{\text{reco}} = 0.78 \pm 0.02$ where the error is statistical only.

The residuals R_θ and R_ϕ, defined separately for θ and ϕ as the difference between the generated and reconstructed angles, include both detector and reconstruction effects. As such, the standard deviation of their distribution can be interpreted as the angular resolution that can be achieved with the complete set up. It is an optimistic view as the simulated data do not contain any noise at this stage. Fig 5 shows the Gaussian fit to both R_θ and R_ϕ. Combining both resolutions on θ and ϕ yields a global value of 6.5 mrad at worst, which is to be compared with typical muon telescopes angular resolution that ranges from a 4 to 10 mrad depending on the muon angle with the telescope aiming line.

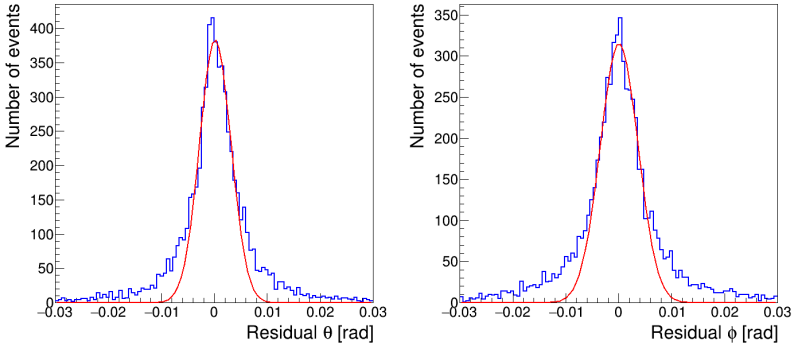

Figure 5: Residual between the muon direction, defined by the angles θ and ϕ, as reconstructed by the algorithm and generated. A Gaussian fit to each distribution is super-imposed in red.

5. Conclusion

In conclusion, we report here the first successful operation of D3DT, the first TPC using a 2D-multiplexed readout plane. An automatized test bench has been developed to allow a precise characterization of the readout plane. This resulted in the identification of a manufacturing error but overall, the uniformity in relative gain and energy resolution are satisfying. Finally a reconstruction algorithm has been tested on simulated data, showing promising performances.

References

[1] H. Gómez et al, 2020 J. Phys.: Conf. Ser. 1498 012047

[2] M. Lehuraux et al., *Automatized characterization of 2D-multiplexed Micromegas detector for muon tomography*, (accepted on 12/10/22), Nuclear Inst. and Methods in Physics Research, A

[3] I. Giomataris et al. (2006), *Micromegas in a bulk*, Nuclear Inst. and Methods in Physics Research, A, 10.1016/J.NIMA.2005.12.222

[4] C. Flouzat et al. (2014), *Dream: a 64-channel front-end chip with analogue trigger latency buffer for the Micromegas tracker of the CLAS12 experiment*, Proc. of TWEPP conference, 10.1016/J.NIMA.2005.12.222

[5] S. Agostinelli et al. (2003), *GEANT4 - A simulation toolkit*, Nuclear Inst. and Methods in Physics Research, A, 10.1016/S0168-9002(03)01368-8

[6] Guan et al. (2015), *A parametrization of the cosmic-ray muon flux at sea-level*, arXiv, 10.48550/ARXIV.1509.06176

[7] Fischler et al. (1981), *Random Sample Consensus: A Paradigm for Model Fitting with Applications to Image Analysis and Automated Cartography*, Association for Computing Machinery, 10.1145/358669.358692